Preprints.org

Article

Not peer-reviewed version

Diverse Co(II) Coordination Polymers with the Same Mixed Ligands: Evaluation for Chemical Stability and Structural Transformation

Chia-Yi Lee , Yu-Hui Ye , Song-Wei Wang , Jhy-Der Chen *

Posted Date: 5 March 2024

doi: 10.20944/preprints202403.0256.v1

Keywords: coordination polymer; crystal structure analysis; structural transformation

Preprints.org is a free multidiscipline platform providing preprint service that is dedicated to making early versions of research outputs permanently available and citable. Preprints posted at Preprints.org appear in Web of Science, Crossref, Google Scholar, Scilit, Europe PMC.

Copyright: This is an open access article distributed under the Creative Commons Attribution License which permits unrestricted use, distribution, and reproduction in any medium, provided the original work is properly cited.

Preprints.org (www.preprints.org) | NOT PEER-REVIEWED | Posted: 5 March 2024 doi:10.20944/preprints202403.0256.v1

Disclaimer/Publisher's Note: The statements, opinions, and data contained in all publications are solely those of the individual author(s) and contributor(s) and not of MDPI and/or the editor(s). MDPI and/or the editor(s) disclaim responsibility for any injury to people or property resulting from any ideas, methods, instructions, or products referred to in the content.

Article

Diverse Co(II) Coordination Polymers with the Same Mixed Ligands: Evaluation for Chemical Stability and Structural Transformation

Chia-Yi Lee, Yu-Hui Ye, Song-Wei Wang and Jhy-Der Chen *

Department of Chemistry, Chung Yuan Christian University, Chung Li, Taoyuan City 320, Taiwan; miss10031031@gmail.com (C.-Y.L.); a4862225@gmail.com (Y.-H.Y.); bvbv20520@gmail.com (S.-W.W.)
* Correspondence: jdchen@cycu.edu.tw; Tel.: +886-3-265-3351

Abstract: Reactions of $Co(OAc)_2 \cdot 4H_2O$, *N,N′*-bis(3-pyridylmethyl)oxalamide (**L**) and 4,4′-sulfonyldibenzoic acid (H_2SDA) afforded four coordination polymers with the same mixed ligands, $\{[Co(\mathbf{L})(SDA)(H_2O)_2]\cdot H_2O\cdot CH_3OH\}_n$, **1**, $\{[Co(\mathbf{L})_{0.5}(SDA)]\cdot 2H_2O\cdot 0.5\mathbf{L}\}_n$, **2**, $\{[Co(\mathbf{L})_{1.5}(SDA)(H_2O)]\cdot H_2O\}_n$, **3**, and $\{[Co_2(\mathbf{L})_{1.5}(SDA)_2(H_2O)_2]\cdot 4H_2O\}_n$, **4**, which have been structurally characterized by using single crystal X-ray crystallography. Complexes **1** – **4** are 2D layers, revealing the topologies of **sql**, 2,6L1, (4,4)Ia and 6L12, respectively, and demonstrating that the metal to ligand ratio, solvent system and reaction temperature are important in determining the structural diversity. Immersion of these complexes into various solvents show that the structural types govern the chemical stabilities of **1** – **4**. Reversible structural transformation can be shown for complexes **1** and **2** upon solvent removal and adsorption, while those of **3** and **4** are irreversible.

Keywords: coordination polymer; crystal structure analysis; structural transformation

1. Introduction

The design and synthesis of functional coordination polymers (CPs) have drawn a great attention of the scientists over the past years, because of their intriguing structures and potential applications in the fields of sensors, gas adsorption and storage, heterogeneous catalysis, magnetism and luminescence [1–10]. The structural diversity of CPs is conditional upon many factors such as the identities of metal ions, linkers and counter ions as well as the reaction conditions involving the metal to ligand ratio, solvent system and reaction condition. Therefore, efforts have been made to employ and control the applicable factors to prepare the target CPs.

Investigations on the structural transformations of CPs are important, because such phenomena show potential applications in switches and sensors [11]. Structural transformations of CPs that lead to the change from one structure to another is difficult in the solid state due to the constrained rearrangement of the ligands. Structural transformation in CPs can be initiated by the removal of solvent, exchange of guest molecules, exposure to reactive vapors and external stimuli such as heat, light, and mechanical energy [12,13]. In spite of some advancement, a great effort remains necessary to improve the capability to predict and control the structural transformation. Structural transformations in flexible bis-pyridyl-bis-amide (bpba)-based CPs supported by the polycarboxylate ligands have been reported [14–16]. To perform the structural transformations upon solvent removal and adsorption for specific CPs with mixed ligands, it is required to prepare more than two CPs with the same metal ion, neutral spacer and polycarboxylate ligands by manipulating the metal to ligand ratio and solvent system as well as the reaction condition.

In this work, we aim to elucidate the factors that govern the structural diversity of Co(II) CPs constructed from *N,N′*-bis(3-pyridylmethyl)oxalamide (**L**) and 4,4′-sulfonyldibenzoic acid (H_2SDA), Figure 1, and to explore the roles of structural diversity in determining the structural transformations. The synthesis and structures of four diverse CPs $\{[Co(\mathbf{L})(SDA)(H_2O)_2]\cdot H_2O\cdot CH_3OH\}_n$, **1**,

© 2024 by the author(s). Distributed under a Creative Commons CC BY license.

{[Co(**L**)$_{0.5}$(SDA)]·2H_2O·0.5**L**}$_n$, **2**, {[Co(**L**)$_{1.5}$(SDA)(H_2O)]·H_2O}$_n$, **3**, and {[Co_2(**L**)$_{1.5}$(SDA)$_2$(H_2O)$_2$]·4H_2O}$_n$, **4**, as well as the evaluation of their chemical stabilities and structural transformations form the subject of this report.

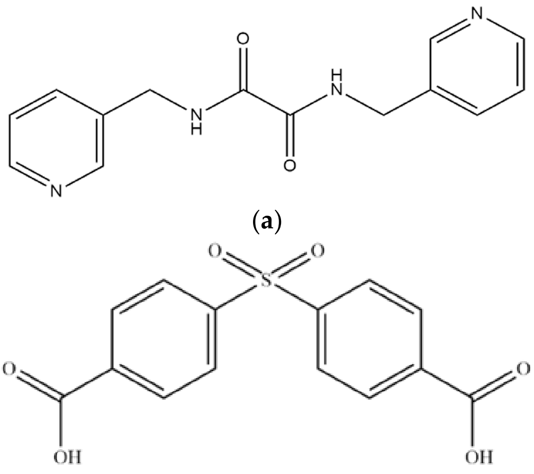

(**a**)

(**b**)

Figure 1. Structures of (**a**) **L** and (**b**) H_2SDA.

2. Results and Discussion

2.1. Preparations for Complexes **1** – **4**

While the procedures in the experimental section afforded the major products 1 – 4, respectively, some minor products can also be obtained. Table 1 lists the reaction conditions as well as their yields, which are dependent on the metal to ligand ratio, solvent system reaction and reaction condition.

Table 1. Synthetic yields for complexes **1** - **4**.

0.20 mmol Co(OAc)$_2$·4H_2O + 0.10 mmol H_2SDA + x L	**Solvent**	**Temperature (°C)/ Time (days)**	**Complex**	**Yield (%)**
x = 0.10 mmol	8 ml H_2O and 2ml MeOH	80 / 2	**1**	33.70
	10 ml H_2O	80 / 2	**2** **3** **4**	3.29 0.0010 13.55
		80 / 4	**2** **4**	2.09 17.34
x = 0.20 mmol		60 / 2	**3**	27.53
		80 / 2	**2** **3** **4**	4.18 9.28 6.45
		80 / 4	**2** **4**	26.21 6.86

2.2. Structure of **1**

Crystals of complex **1** conform to the triclinic space group $P\bar{1}$ and each asymmetric unit consists of one Co(II) ion, one **L** ligand, one SDA^{2-} ligand, two coordinated water molecules, one cocrystallized water molecule and one cocrystallized MeOH molecule. Figure 2a shows the coordination

Preprints.org (www.preprints.org) | NOT PEER-REVIEWED | Posted: 5 March 2024 doi:10.20944/preprints202403.0256.v1

environment about the Co(II) metal center, which is six-coordinated by two nitrogen atoms from the two **L** ligands [Co-N = 2.1500(16) - 2.1503(16) Å], two oxygen atoms from two SDA^{2-} ligands [Co-O = 2.0225(14) - 2.0569(13) Å] and two oxygen atoms from the two coordination water molecules [Co-O = 2.1256(14) - 2.1549(16) Å], resulting in a distorted octahedral geometry. The Co(II) central metal atoms are bridged by SDA^{2-} and **L** ligands to form a 2D layer. Topologically, if the Co(II) atoms are regarded as 4-connected nodes and the SDA^{2-} ligands as 2-connected nodes, while the **L** ligands as linkers, the structure of **1** can be simplified as 2,4-connected 2D net with the (6^4·8·10)(6)-2,4L3 topology, Figure 2b. Moreover, if the SDA^{2-} ligands are considered as linkers, the structure of **1** can be further simplified as a 4-connected 2D net with the (4^4·6^2)-**sql** topology, Figure 2c, determined by using ToposPro program [17].

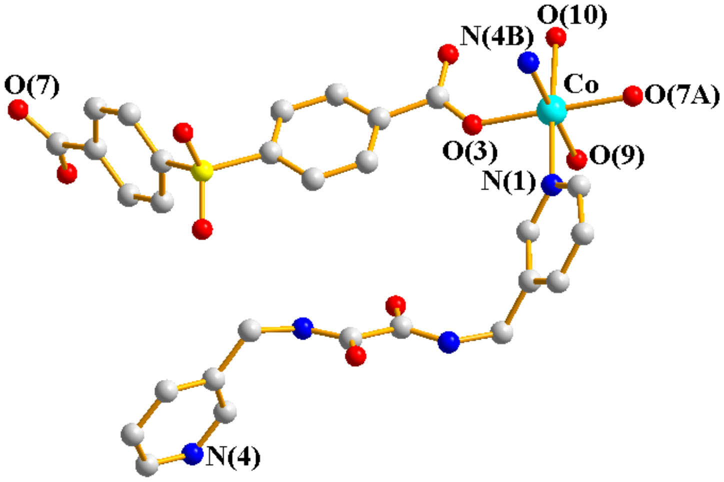

(**a**)

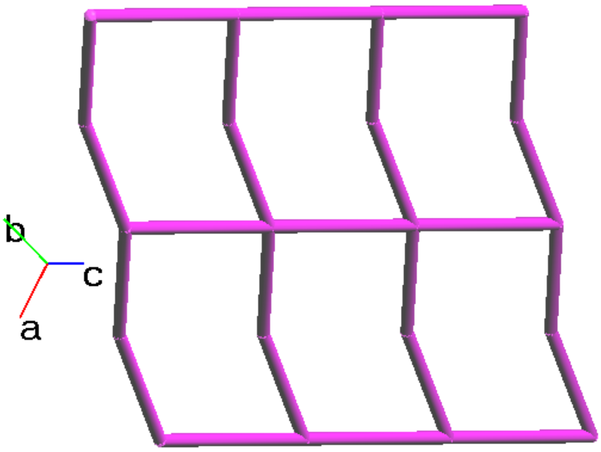

(**b**)

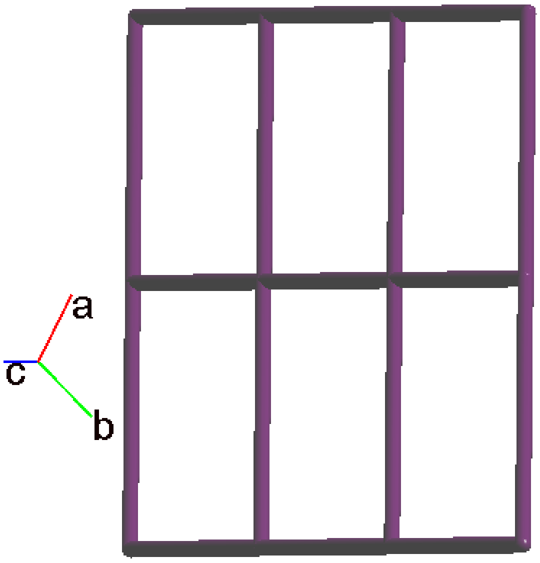

(c)

Figure 2. (**a**) Coordination environment of Co(II) ion in **1**. Symmetry transformations used to generate equivalent atoms: (A) x - 1, y, z – 1; (B) x, y, z – 1; (C) x + 1, y, z + 1; (D) x, y, z + 1. (**b**) Topological structure of **1** with the $(6^{4}\cdot 8\cdot 10)(6)$-2,4L3 topology. (**c**) Topological structure of **1** with the $(4^{4}\cdot 6^{2})$-**sql** topology.

2.3. *Structure of* 2

Crystals of complex **2** conform to the triclinic space group $P\bar{1}$ and each asymmetric unit consists of one Co(II) ion, a half of an **L** ligand, one SDA^{2-} ligand, two cocrystallized water molecules and a half of a cocrystallized **L** ligand. Figure 3a shows the coordination environment about Co(II) metal centers, which are five-coordinated by two nitrogen atoms from the two **L** ligands [Co-N = 2.0600(13) Å] and four oxygen atoms from four SDA^{2-} ligands [Co-O = 2.0140(11) - 2.0649(11) Å], resulting in distorted square pyramidal geometries. The Co(II) central metal atoms are bridged by SDA^{2-} ligands to form dinuclear Co(II) units [Co---Co = 2.7202(8) Å], which are further extended by **L** ligands to form a 2D layer. Topologically, if the Co(II) ions are regarded as 5-connected nodes and the SDA^{2-} as 4-connected nodes, while the **L** ligands as linkers, the structure of **2** can be simplified as a 4,5-connected net with the $(4^{6}\cdot 6^{4})(4^{6})$-4,5L51 topology (standard representation), as illustrated in Figure 3b. If the dinuclear Co(II) units are regarded as 6-connected nodes and the SDA^{2-} ligands as 2-connected nodes, while the **L** ligands as linkers, the structure of **2** can be simplified as a 2,6-connected net with the $(4^{2}\cdot 6^{8}\cdot 8\cdot 10^{4})(4)_{2}$-2,6L1 topology (cluster representation), as illustrated in Figure 3c.

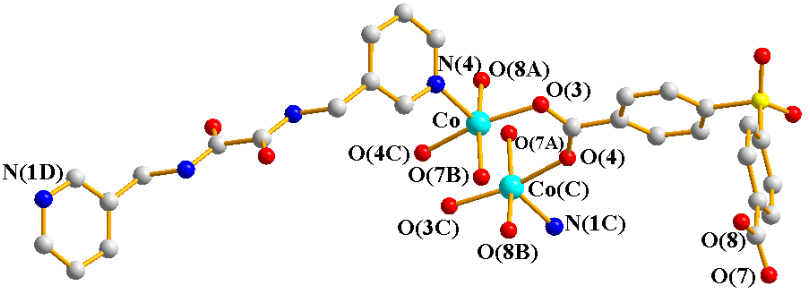

(a)

Preprints.org (www.preprints.org) | NOT PEER-REVIEWED | Posted: 5 March 2024 doi:10.20944/preprints202403.0256.v1

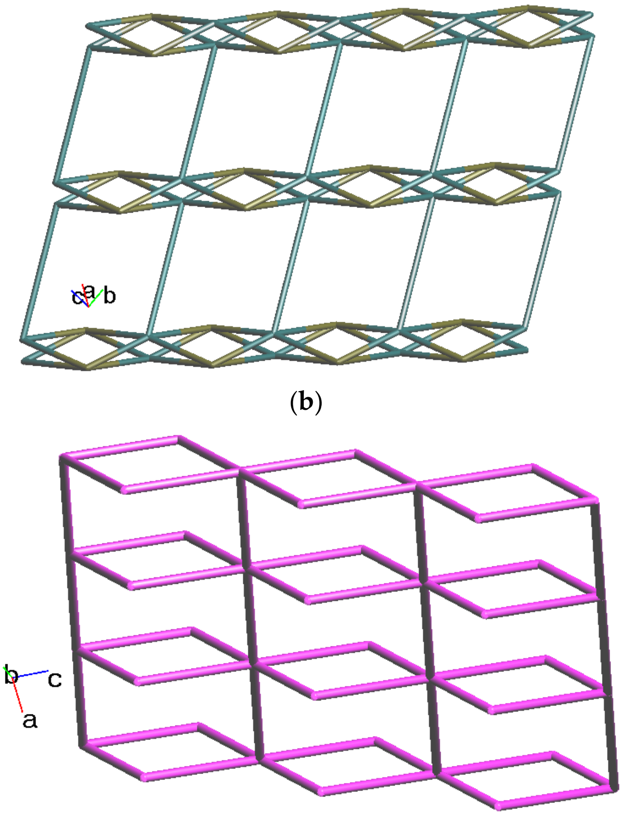

(**b**)

(**c**)

Figure 3. (**a**) Coordination environment of Co(II) ion in **2**. Symmetry transformations used to generate equivalent atoms: (A) x, y + 1, z – 1; (B) -x, -y, -z + 2; (C) -x, -y + 1, -z + 1; (D) -x + 1, -y + 2, -z + 1; (E) -x, -y + 2, -z; (F) x, y- 1, z + 1. (**b**) Topological structure of **2** showing the $(4^6{\cdot}6^4)(4^6)$- 4,5L51 topology. (**c**) Topological structure of **2** showing the $(4^2{\cdot}6^8{\cdot}8{\cdot}10^4)(4)_2$-2,6L1 topology.

2.4. Structure of **3**

Crystals of **3** conform to the triclinic space group $P\bar{1}$ and each asymmetric unit consists of one Co(II) ion, one and a half of an **L** ligand, one SDA^{2-} ligand, one coordinated water molecule and one cocrystallized water molecule. Figure 4a shows the coordination environment about Co(II) metal center, which is six-coordinated by three nitrogen atoms from the three **L** ligands [Co-N = 2.168(3) - 2.228(3) Å], two oxygen atoms from two SDA^{2-} ligands [Co-O = 2.038(2) and 2.053(2) Å] and one oxygen atom from the coordinated water molecule [Co-O = 2.144(2) Å], resulting in a distorted octahedral geometry. The Co(II) central metal atoms are bridged by SDA^{2-} and **L** ligands to form a 2D layer. Topologically, if the Co(II) atoms are regarded as 5-connected nodes and the SDA^{2-} ligands as 2-connected nodes, while the **L** ligands as linkers, the structure of **3** can be simplified as a 2,5-connected net with the $(4^2{\cdot}6^7{\cdot}10)(6)$ topology, Figure 4b. Moreover, if the SDA^{2-} ligands are considered as linkers, the structure of **3** can be further simplified as a 5-connected net with the $(4^8{\cdot}6^2)$-(4,4)Ia topology, as illustrated in Figure 4c.

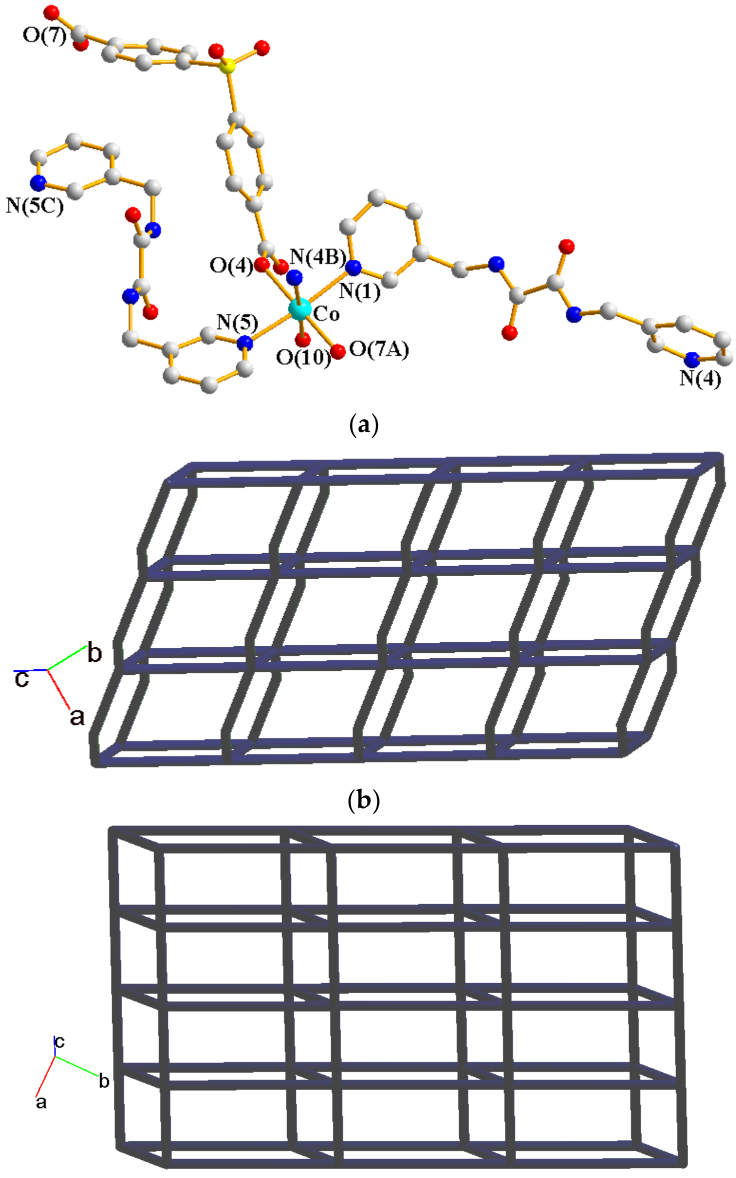

(**a**)

(**b**)

(**c**)

Figure 4. (**a**) Coordination environment of Co(II) ion in **3**. Symmetry transformations used to generate equivalent atoms: (A) x, y + 1, z + 1; (B) x, y, z – 1; (C) -x + 1, -y + 2, -z; (D) x, y - 1, z – 1; (E) x, y, z + 1. (**b**) Topological structure of **3** with the ($4^2{\cdot}6^7{\cdot}10$)(6) topology. (**c**) Topological structure of **3** with the ($4^8{\cdot}6^2$)-(4,4)Ia topology.

2.5. *Structure of* **4**

Crystals of **4** conform to the triclinic system with the $P\bar{1}$ space group. The asymmetric unit contains of two Co(II) ions, one and a half of an **L** ligand, two SDA^{2-} ligands, two coordinated water molecules and four cocrystallized water molecules. Figure 5a exhibits the coordination environment around Co(II) ions. While Co(1) is six-coordinated by one pyridyl nitrogen atom from **L** ligand [Co-N = 2.133(3) Å], two oxygen atoms from two SDA^{2-} ligands [Co-O = 2.054(2) - 2.118(3) Å] and one oxygen from the water molecule [Co-O = 2.147(2) Å], the Co(2) is six-coordinated by two pyridyl nitrogen atoms from the **L** ligand [Co-N = 2.167(3) - 2.172(3) Å], two oxygen atoms from two SDA^{2-} ligands [Co-O = 2.063(3) - 2.069(2) Å] and two oxygen atoms from two water molecules [Co-O = 2.118(3) - 2.134(2) Å], resulting in distorted octahedral geometries. The Co(II) ions are bridged by the SDA^{2-} to form dinuclear units [Co---Co = 3.6113(7) Å], which are further extended by L to form a 2D layer.

Topologically, if the Co(II) ions are considered as 5- and 6-connected nodes and the SDA^{2-} ligands as 2- and 4-connected nodes, whereas the **L** ligands as linkers, the structure of **4** can be simplified as a 2,4,5,6-connected 2D net with the $(3^2{\cdot}4{\cdot}5{\cdot}6^5{\cdot}7)(3^2{\cdot}4^2{\cdot}5^2{\cdot}6^3{\cdot}7^2{\cdot}8^4)(3^2{\cdot}6^2{\cdot}7^2)(4)$ topology, showing cycle self-crossings (standard representation with 2-connected nodes), as shown in Figure 5b. If the 2-connected nodes of SDA^{2-} ligands are considered as linkers, the structure of **4** can be simplified as a 4,5-connected 2D net with the $(3^2{\cdot}4^2{\cdot}6^6)_2(3^2{\cdot}6^2{\cdot}7^2)$ topology with crossing edges (standard representation without 2-connected nodes), as shown in Figure 5c. If the Co(II) dinuclear units are considered as 7-connected nodes and the SDA^{2-} ligands as 2-connected nodes, whereas the **L** ligands as linkers, the structure of **4** can be simplified as a 2,2,7-connected 2D net with the $(4^3{\cdot}5^5{\cdot}6^8{\cdot}8^4{\cdot}10)(4)(6)$ topology (cluster representation with 2-connected nodes), as shown in Figure 5d. If the SDA^{2-} ligands are further considered as linkers, the structure of **4** can be simplified as a 6-connected 2D net with the $(4^{14}{\cdot}6)$-6L12 topology (cluster representation without 2-connected nodes), Figure 5e. Complex **4** can thus be considered as a self-catenated CP.

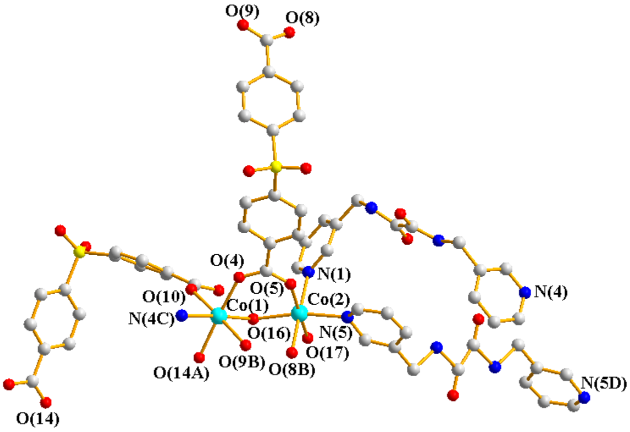

(**a**)

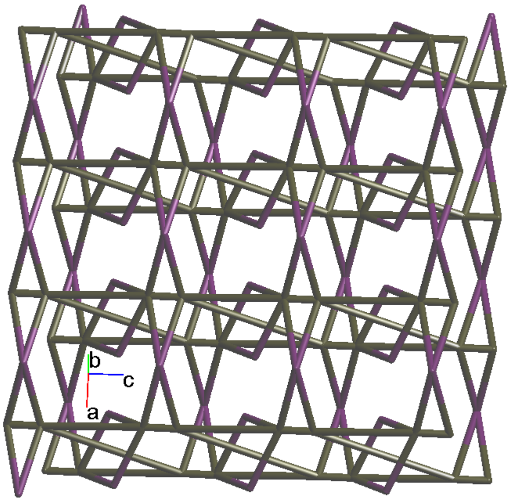

(**b**)

Preprints.org (www.preprints.org) | NOT PEER-REVIEWED | Posted: 5 March 2024

doi:10.20944/preprints202403.0256.v1

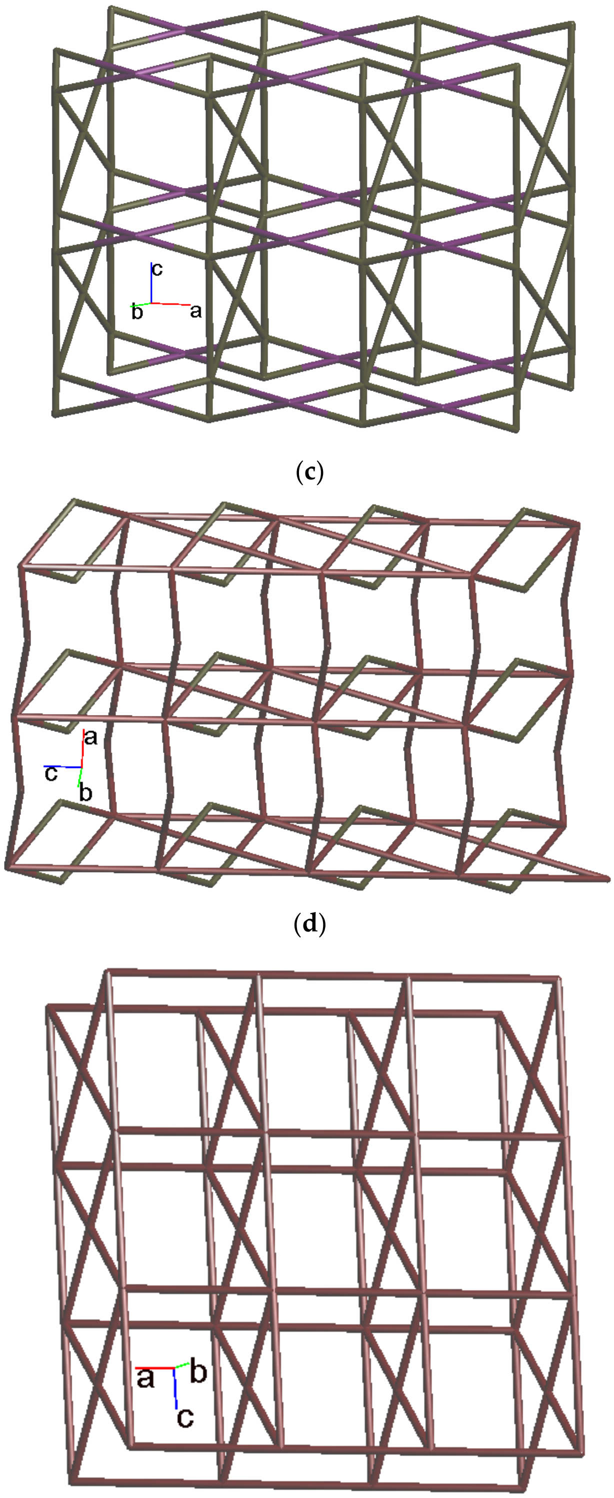

(c)

(d)

(e)

Figure 5. (**a**) Coordination environment of Co(II) ion in **4**. Symmetry transformations used to generate equivalent atoms: (A) -x + 2, -y + 1, -z – 1; (B) x + 1, y, z; (C) x, y, z – 1; (D) -x + 2, -y + 1, -z + 1; (E) x - 1, y, z; (F) x, y, z + 1. (b) Topological structure with the $(3^2{\cdot}4{\cdot}5{\cdot}6^5{\cdot}7)(3^2{\cdot}4^2{\cdot}5^2{\cdot}6^3{\cdot}7^2{\cdot}8^4)(3^2{\cdot}6^2{\cdot}7^2)(4)$ topology. (c) Topological structure with the $(3^2{\cdot}4^2{\cdot}6^6)_2(3^2{\cdot}6^2{\cdot}7^2)$ topology. (d) Topological structure with the $(4^3{\cdot}5^5{\cdot}6^8{\cdot}8^4{\cdot}10)(4)(6)$ topology. (e) Topological structure with the $(4^{14}{\cdot}6)$- 6L12 topology.

Preprints.org (www.preprints.org) | NOT PEER-REVIEWED | Posted: 5 March 2024 doi:10.20944/preprints202403.0256.v1

2.6. Ligand Conformations and Coordination Modes

For the ligand *N,N′*-bis(3-Pyridylmethyl)oxalamide (**L**), the positions of the two C=O groups can be distinguished as *trans* or *cis*. When the two groups of C=O groups show opposite directions, it is defined as *trans*, and when they show the same direction, it is *cis*. Because of the different orientations adopted by the pyridyl nitrogen atoms and the amide oxygen atoms, three more conformations can be expressed as anti-anti, syn-anti and syn-syn. Accordingly, the ligand conformations of **L** in **1** – **4** are listed in Table 2, as well as the coordination modes of the SDA^{2-} ligands. Moreover, while the **L** ligands in **1** - **4** coordinate to the metal centers through the two pyridyl nitrogen atoms, the SDA^{2-} ligands bridge two and four metal atoms.

Table 2. Ligand conformations and bonding modes of complexes **1**–**4**.

	Ligand Conformation	Coordination Mode
1	 *trans syn-syn*	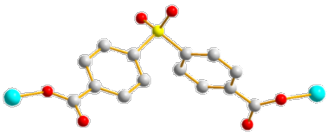 μ_2-κO:κO′
2	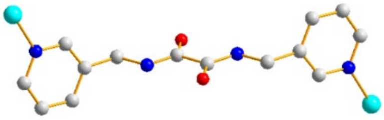 *trans syn-syn*	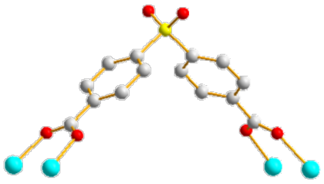 μ_4-κO:κO′: κO′′:κO′′′
3	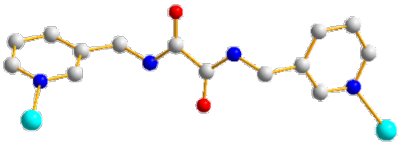 *trans anti-syn*	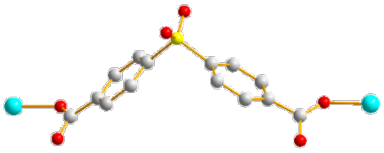 μ_2-κO:κO′
4	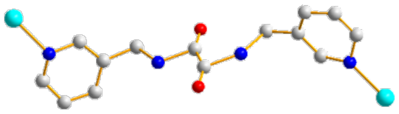 *trans syn-syn*	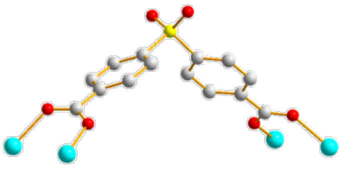 μ_4-κO:κO’:κO”:κO”’
	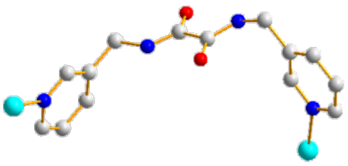 *trans anti-syn*	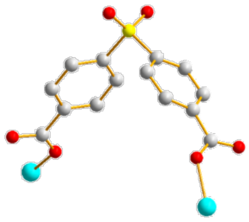 μ_2-κO:κO’

2.7. Powder X-ray Analysis

In order to check the bulk purities of the products, powder X-ray diffraction (PXRD) experiments have been carried out for complexes **1** - **4**. As shown in Figures S1–S4, the peak positions of the experimental and simulated PXRD patterns are in agreement with each other, which demonstrate that the crystal structures are truly representative of the bulk materials.

Preprints.org (www.preprints.org) | NOT PEER-REVIEWED | Posted: 5 March 2024 doi:10.20944/preprints202403.0256.v1

2.8. Thermal Properties

Thermal gravimetric analysis (TGA) was carried out to examine the thermal decomposition of the four complexes. The samples were recorded from about 30 to 800 °C at 10 °C min^{-1} under a N_2 atmosphere, Table 3 and Figures S5–S8. Two-step decomposition was observed for the complexes, revealing that the decomposition temperatures for complexes **1** – **4** are in the range 200 – 300 °C.

Table 3. Thermal properties of complexes **1**–**4**.

Complex	Weight Loss of Solvent °C (Calc/Found), %	Weight Loss of Ligand °C (Calc/Found), %
1	3H2O + MeOH ~ 170 (11.95/9.23)	**L** + (SDA^{2-}) 290 - 800 (80.06/82.72)
2	2 H2O ~ 130 (5.38/4.65)	**L** + (SDA^{2-}) 270 - 800 (86.02/88.15)
3	2 H2O ~ 170 (4.48/4.56)	1.5 **L** + (SDA^{2-}) 200 - 800 (88.36/85.91)
4	6 H2O ~ 130 (8.71/8.23)	1.5 **L** + 2 (SDA^{2-}) 300 - 800 (82.02/78.76)

2.9. Chemical Stabilities

To check the chemical stabilities of complexes **1** - **4** in the various solvents, 10 mg of each complex was immersed into 10 mL of methanol (MeOH), ethanol (EtOH), ether, hexane, tetrahydrofuran (THF), acetonitrile (ACN), dichloromethane (DCM), dimethylacetamide (DMAC) and dimethylformamide (DMF), respectively, for a week, which were then filtered and dried at room temperature. The PXRD patterns, Figures S9–S12, show that complex **4** is unstable in all of the solvents and complex **1** is stable in EtOH, ACN and DCM, whereas complex **2** is stable in ether, hexane and ACN and complex **3** is stable in EtOH, ether, hexane, THF, ACN and DCM, indicating that the structural diversity is important in determining the chemical stability of the Co(II) CPs comprising **L** and SDA^{2-} ligands.

2.10. Attempts for Structural Transformation

Complexes **1** - **4** provide an opportunity for the investigation of structural transformation due to the solvent exchange because they comprise the same metal centers and organic ligands with different metal to ligand ratios. To investigate the structural transformations, complexes **1** – **4** were first heated at 110, 130, 170 and 130 °C, respectively, for two hours to obtain fully desolvated samples. Figure S13 depicts the colors of these complexes before and after heating. The PXRD patterns, Figures S14–S17, demonstrate the structures of these desolvated complexes are different from the original ones upon removal of the crystallized solvents. Moreover, the desolvated product of **1** shows reversible structural transformations in MeOH, EtOH and ACN and that of **2** shows reversible structural transformations in ether and DMAc solution. However, desolvated samples of **3** and **4** in the solvents remain intact.

Complexes **1**, **3** and **4** were all soluble in water, while complex **2** was slightly soluble in water. To investigate the stabilities of these complexes in water, complexes **1** – **4** were immersed into water for **2** days and then the water evaporated to afford solid samples. Their PXRD patterns and photos, Figures 6 and 7, show that complexes **1**, **3** and **4**, and part of complex **2** were probably transformed into the same new complex. Their IR spectra confirm this change, Figure S18. Figure 7 depicts a drawing that summarizes the reaction pathways and the colors of the complexes.

Preprints.org (www.preprints.org) | NOT PEER-REVIEWED | Posted: 5 March 2024 doi:10.20944/preprints202403.0256.v1

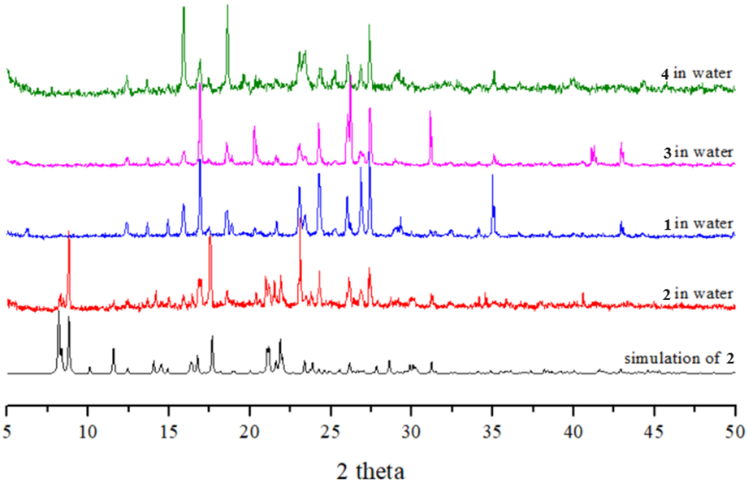

Figure 6. PXRD patterns and photos of complexes 1 - 4 after immersion in water.

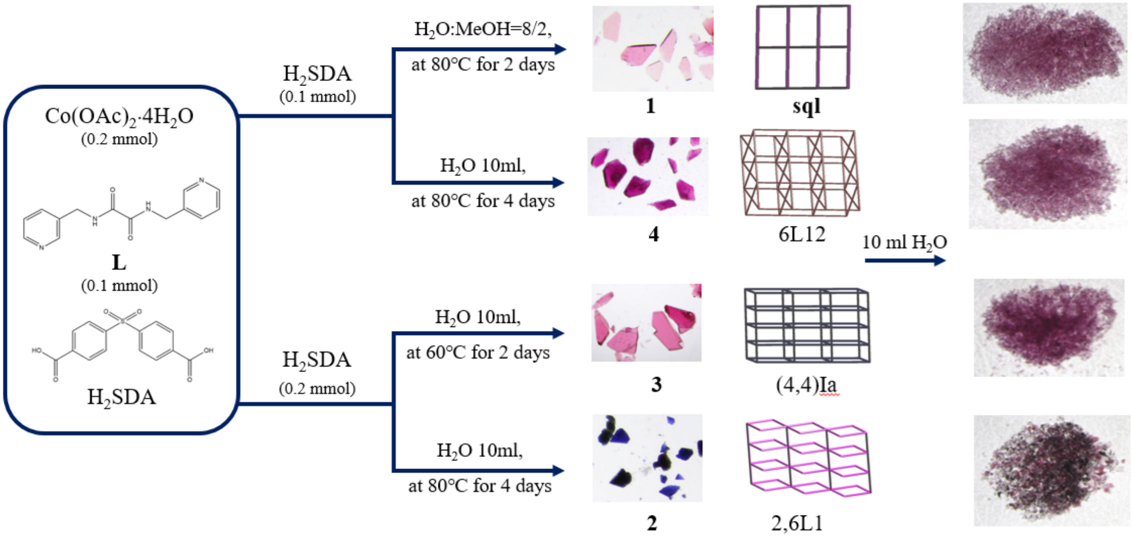

Figure 7. A drawing showing the reaction pathways and the colors of the complexes.

3. Materials and Methods

3.1. General Procedures

Elemental analyses were performed on a PE 2400 series II CHNS/O elemental analyzer (PerkinElmer instruments, Shelton, CT, USA). Infrared spectra were obtained from a JASCO FT/IR-460 plus spectrometer with pressed KBr pellets (JASCO, Easton, MD, USA). Powder X-ray diffraction patterns were carried out with a Bruker D8-Focus Bragg–Brentano X-ray powder diffractometer equipped with a CuK*α* ($\lambda\alpha$ = 1.54178 Å) radiation (Bruker Corporation, Karlsruhe, Germany). Thermal gravimetric analyses (TGA) were carried out on a TG/DTA 6200 analyzer (SEIKO Instruments Inc., Chiba, Japan).

Materials

The reagent $Co(OAc)_2{\cdot}4H_2O$ was purchased from Alfa Aesar (Ward Hill, MA, USA), and H_2SDA from Aldrich Chemical Co. (St. Louis, MO, USA). The ligands N,N′-di(3-methylpyridyl)oxalamide (**L**) was prepared according to a published procedure [18].

Preprints.org (www.preprints.org) | NOT PEER-REVIEWED | Posted: 5 March 2024

doi:10.20944/preprints202403.0256.v1

3.2. Preparations

3.2.1. {[Co(**L**)(SDA)(H_2O)$_2$]·H_2O·CH_3OH}$_n$, **1**

A mixture of Co(OAc)$_2$·4H_2O (0.050 g, 0.20 mmol), **L** (0.027 g, 0.10 mmol) and H_2SDA (0.031, 0.10 mmol) were placed in a 23 mL Teflon reaction flask containing 8 mL H_2O and 2 mL MeOH, which was sealed and heated at 80 °C for 48 h under autogenous pressure and then the reaction system was cooled to room temperature at a rate of 2 °C per hour. The dark pink crystals suitable for single-crystal X-ray diffraction were obtained. Yield: 0.049 g (34 %). Anal. Calcd for $C_{29}H_{32}CoN_4O_{12}S$ (MW = 719.57): C, 48.40; H, 4.48; N, 7.79 %. Found: C, 48.31; H, 4.11; N, 8.04 %. FT-IR (cm^{-1}): 3677 (m), 3504 (m), 3327 (w), 3060 (w), 1663 (s), 1599 (s), 1557 (m), 1512 (m), 1385 (s), 1295 (m), 1159 (s), 1102 (m), 1036 (w), Figure S19.

3.2.2. {[Co(**L**)$_{0.5}$(SDA)]·2H_2O·0.5L}$_n$, **2**

Complex **2** was prepared by following similar procedures for **1**, except that a mixture of Co(OAc)$_2$·4H_2O (0.050 g, 0.20 mmol), **L** (0.054 g, 0.20 mmol) and H_2SDA (0.031, 0.10 mmol) in 10 mL H_2O was heated at 80 °C for 96 h. Indigo crystals were obtained. Yield: 0.035 g (26 %). Anal. Calcd for $C_{28}H_{26}CoN_4O_{10}S$ (MW = 669.52): C, 50.23; H, 3.91; N, 8.37 %. Found: C, 50.50; H, 3.73; N, 8.29 %. FT-IR (cm^{-1}): 3504 (m), 3048 (w), 2944 (w), 1654 (s), 1597 (s), 1507 (s), 1404 (s), 1291 (m), 1227 (m), 1168 (m), 1103 (m), 1034 (m), Figure S20.

3.2.3. {[Co(**L**)$_{1.5}$(SDA)(H_2O)]·H_2O}$_n$, **3**

Complex **3** was prepared by following similar procedures for **1**, except that a mixture of Co(OAc)$_2$·4H_2O (0.050 g, 0.20 mmol), **L** (0.054 g, 0.20 mmol) and H_2SDA (0.031, 0.10 mmol) in 10 mL H_2O was heated at 60 °C for 48 h. Dark pink crystals were obtained. Yield: 0.039 g (28 %). Anal. Calcd for $C_{35}H_{33}CoN_6O_{11}S$ (MW = 804.66): C, 52.24; H, 4.13; N, 10.44 %. Found: C, 52.31; H, 3.94; N, 10.27 %. FT-IR (cm^{-1}): 3501 (w), 3394 (w), 3333 (w), 3275 (w), 1658 (s), 1599 (s), 1512 (s), 1393 (m), 1382 (m), 1102 (m), 1034 (m), Figure S21.

3.2.4. {[Co_2(**L**)$_{1.5}$(SDA)$_2$(H_2O)$_2$]·4H_2O}, **4**

Complex **4** was prepared by following similar procedures for **1**, except that a mixture of Co(OAc)$_2$·4H_2O (0.050 g, 0.20 mmol), **L** (0.027 g, 0.10 mmol) and H_2SDA (0.031, 0.10 mmol) in 10 mL H_2O was heated at 80 °C for 96 h. Violet crystals were obtained. Yield: 0.022 g (17 %). Anal. Calcd for $C_{49}H_{49}Co_2N_6O_{21}S_2$ (MW = 1239.92): C, 47.46; H, 3.98; N, 6.78 %. Found: C, 47.77; H, 3.69; N, 6.80 %. FT-IR (cm^{-1}): 3503 (w), 2816 (w), 1662 (w), 1596 (s), 1514 (m), 1384 (m), 1351 (w), 1292 (m), 1228 (w), 1160 (m), 1100 (m), 1034 (w), Figure S22.

3.3. X-ray Crystallography

Single crystal X-ray data of complexes **1** - **4** were collected by using a Bruker AXS SMART APEX II CCD diffractometer, equipped with a graphite-monochromated MoKα radiation (0.71073 Å), which were then reduced by using standard methods [19], followed by empirical absorption corrections based on a "multi-scan". Direct or Patterson method was adopted to locate the positions of some of the heavier atoms, and the remaining atoms were established in a series of alternating difference Fourier maps and least-square refinements. Except the hydrogen atoms of the water molecules, those of the others were added by using the HADD command in SHELXTL 6.1012 [20]. Table 4 lists the crystal and structure refinement parameters for **1–4**. The CCDC no. 2330673-2330676 contain the supplementary crystallographic data for this paper. These data can be obtained free of charge via http://www.ccdc.cam.ac.uk/conts/retrieving.html or from the Cambridge Crystallographic Data Centre, 12 Union Road, Cambridge CB2 1EZ, UK; fax: +44 1223 336 033; e-mail: deposit@ccdc.cam.ac.uk; or at http://www.ccdc.cam.ac.uk.

Table 4. Crystal data for complexes **1–4.**

Complex	1	2	3	4
Formula	$C_{29}H_{32}CoN_4O_{12}S$	$C_{28}H_{26}CoN_4O_{10}S$	$C_{35}H_{33}CoN_6O_{11}S$	$C_{49}H_{49}Co_2N_6O_{21}S_2$
Formula weight	719.57	669.52	804.66	1239.92
Crystal system	Triclinic	Triclinic	Triclinic	Triclinic
Space group	$P\bar{1}$	$P\bar{1}$	$P\bar{1}$	$P\bar{1}$
a, Å	12.0281(8)	10.537(3)	11.6913(8)	13.9967(9)
b, Å	12.3628(9)	12.378(2)	12.5564(8)	14.4949(8)
c, Å	12.5821(9)	12.849(2)	13.2862(8)	14.9094(8)
α, °	110.490(3)	61.476(8)	105.7159(18)	104.0893(14)
β, °	99.692(3)	72.697(10)	105.6037(18)	93.1620(15)
γ,°	108.754(3)	85.374(14)	91.3885(19)	114.1365(14)
V, $Å^3$	1574.1(2)	1402.0(5)	1798.4(2)	2636.1(3)
Z	2	2	2	2
D_{calc}, Mg/m^3	1.518	1.586	1.486	1.562
F(000)	746	690	832	1278
μ(Mo K$_\alpha$), mm^{-1}	0.682	0.754	0.605	0.795
Independent reflection	7756 [R(int) = 0.0276]	6938 [R(int) = 0.0202]	7082 [R(int) = 0.1016]	10361 [R(int) = 0.0473]
Data/restraint/parameter	7756 / 0 / 452	6938 / 0 / 397	7082 / 0 / 497	10361 / 2 / 776
quality-of-fit indicator [c]	1.048	1.063	1.004	1.019
Final R indices [I > 2σ(I)] [a,b]	R1 = 0.0413, wR2 = 0.1070	R1 = 0.0296, wR2 = 0.0825	R1 = 0.0535, wR2 = 0.0871	R1 = 0.0495, wR2 = 0.1133
R indices (all data)	R1 = 0.0440, wR2 = 0.1089	R1 = 0.0323, wR2 = 0.0841	R1 = 0.1193, wR2 = 0.1061	R1 = 0.0811, wR2 = 0.1364

[a] $R_1 = \Sigma||F_o| - |F_c||/\Sigma|F_o|$. [b] $wR_2 = [\Sigma w(F_o^2 - F_c^2)^2/\Sigma w(F_o^2)^2]^{1/2}$. $w = 1/[\sigma^2(F_o^2) + (ap)^2 + (bp)]$. $p = [\max(F_o^2 \text{ or } 0) + 2(F_c^2)]/3$. a = 0.0477, b = 2.2049 for **1**; a = 0.0411, b = 1.2183 for **2**; a = 0.0299, b = 0.9541 for **3**; a = 0.04854, b = 5.8594 for **4**. [c] quality of fit = $[\Sigma w(|F_o^2| - |F_c^2|)^2/N_{observed} - N_{parameters})]^{1/2}$.

4. Conclusions

By careful evaluation of the metal to ligand ratio, solvent system and reaction temperature, four diverse CPs constructed from Co(II) salts, *N,N′*-bis(3-pyridylmethyl)oxalamide (**L**) and 4,4′-sulfonyldibenzoic acid (H_2SDA) have been successfully accomplished, which display 2D layers with the **sql**, 2,6L1, (4,4)Ia and 6L12 topologies, respectively. It has also been shown that the structural diversity is important in determining the chemical stabilities of complexes **1** - **4**. Reversible structural transformations were observed for complexes **1** and **2** upon solvent removal and adsorption, while those of **3** and **4** are irreversible. Moreover, complexes **1 – 4** decompose in water and may afford the identical product. Complexes **1 – 4** represent a unique example of four Co(II) CPs with **L** and SDA^{2-} ligands that have been structurally characterized. For a comparison, it is interesting to note that five Cd(II) CPs containing 1,4-bis(2-methyl-imidazol-1-yl)butane and 5-bromoisophthalate ligands have been reported [21].

Supplementary Materials: The following supporting information can be downloaded at the website of this paper posted on Preprints.org.

Author Contributions: Investigation, C.-Y.L.; data curation, Y.-H.Y. and S.-W.W.; review and supervision, J.-D.C. All authors have read and agreed to the published version of the manuscript.

Funding: This research was funded by the National Science and Technology Council of the Republic of China: NSTC 112-2113-M-033-004.

Institutional Review Board Statement: Not applicable.

Informed Consent Statement: Not applicable.

Data Availability Statement: Data are contained within the article or Supplementary Materials.

Acknowledgments: We are grateful to the National Science and Technology Council of the Republic of China for support.

Conflicts of Interest: The authors declare no conflicts of interest.

References

1. Tiekink, E.R.; Vittal, J.J. *Frontiers in Crystal Engineering*; John Wiley & Sons: West Sussex, England, 2006.
2. Batten, S.R.; Neville, S.M.; Turner, D.R. *Coordination Polymers Design, Analysis and Application*; The Royal Society of Chemistry: London, UK, 2009.
3. Lustig, W.P.; Mukherjee, S.; Rudd, N.D.; Desai, A.V.; Li, J.; Ghosh, S.K. Metal-organic frameworks: Functional luminescent and photonic materials for sensing applications. *Chem. Soc. Rev.* **2017**, *46*, 3242−3285.
4. Shi, Y.X.; Zhang, W.H.; Abrahams, B.F.; Braunstein, P.; Lang, J.P. Fabrication of Photoactuators: Macroscopic Photomechanical Responses of Metal-Organic Frameworks to Irradiation by UV Light. *Angew. Chem. Int. Ed.* **2019**, *58*, 9453−9458.
5. Shi, Y.X.; Chen, H.H.; Zhang, W.H.; Day, G.S.; Lang, J.P.; Zhou, H.C. Photoinduced nonlinear contraction behavior in metalorganic frameworks. *Chem. Eur. J.* **2019**, *25*, 8543−8549.
6. Wales, D.J.; Grand, J.; Ting, V.P.; Burke, R.D.; Edler, K.J.; Bowen, C.R.; Mintova, S.; Burrows, A.D. Gas sensing using porous materials for automotive applications. *Chem. Soc. Rev.* **2015**, *44*, 4290−4321.
7. Li, B.; Wen, H.-M.; Cui, Y.; Zhou, W.; Qian, G.; Chen, B. Emerging Multifunctional Metal-Organic Framework Materials. *Adv. Mater.* **2016**, *28*, 8819−8860.
8. Pamela, B.S.; Chen, H.-T.; Lin, C.-H. De novo synthesis and particle size control of iron metal organic framework for diclofenac drug delivery. *Microporous Mesoporous Mater.* **2020**, *309*, 110495.
9. Ma, L.; Abney, C.; Lin, W. Enantioselective catalysis with homochiral metal–organic frameworks. *Chem. Soc. Rev.* **2009**, *38*, 1248−1256.
10. Pamei, M.; Puzari, A. Luminescent transition metal–organic frameworks: An emerging sensor for detecting biologically essential metal ions. *Nano-Struct. Nano-Objects* **2019**, *19*, 100364.
11. Vittal, J.J. Supramolecular structural transformations involving coordination polymers in the solid state. *Coord, Chem. Rev.* **2007**, *251*, 1781-1795.
12. Kole, G. K.; Vittal, J.J. Solid-state reactivity and structural transformations involving coordination polymers. *Chem. Soc. Rev.* **2013**, *42*, 1755-1775.
13. Chakraborty, S.; Park, I.-H.; Medishetty, R.; Vittal, J.J. Two-Dimensional Metal-Organic Framework Materials: Synthesis, Structures, Properties and Applications. *Chem. Rev.* **2021**, *121*, 3751–3891.
14. Liu, Y.-F.; Hu, J.-H.; Lee, W.-T.; Yang, X.-K.; Chen, J.-D. Structural Transformations of Cobalt(II) Coordination Polymers Constructed from *N,N′*-Di-3-pyridyladipoamide and Tetracarboxylic Acids: Disentanglement upon Water Coordination. *Cryst. Growth Des.* **2020**, *20*, 7211–7218.
15. Yang, X.-K.; Chen, J.-D. Crystal-to-crystal transformation and linker exchange in Cd(II) coordination polymers based on flexible bis-pyridyl-bis-amide and 1,4-naphthalenedicarboxylate. *CrystEngComm* **2019**, *21*, 7437-7446.
16. Hsu, C.-H.; Huang, W.-C.; Yang, X.-K.; Yang, C.-T.; Chhetri, P. M.; Chen, J.-D. Entanglement and Irreversible Structural Transformation in Co(II) Coordination Polymers Based on Isomeric Bis-pyridyl-bis-amide Ligands. *Cryst. Growth Des.* **2019**, *19*, 1728-1737.
17. Blatov, V.A.; Shevchenko, A.P.; Proserpio, D.M. Applied topological analysis of crystal structures with the program package TopospPro. *Cryst. Growth Des.* **2014**, *14*, 3576–3586.
18. Lee, W.T.; Liao, T.T.; Chen, J.-D. Nickel (II) Coordination Polymers Supported by Bis-pyridyl-bis-amide and Angular Dicarboxylate Ligands: Role of Ligand Flexibility in Iodine Adsorption. *Int. J. Mol. Sci.* **2022**, *23*, 3603.
19. Bruker, A.X.S. *APEX2, V2008.6, SADABS V2008/1, SAINT V7.60A, SHELXTL V6.14*; Bruker AXS Inc.: Madison, WI, USA, 2008.
20. Sheldrick, G.M. Crystal structure refinement with SHELXL. *Acta Crystallogr.* **2015**, *C71*, 3–8.
21. Hou, Y.-F.; Liu, B.; Yue, K.-F.; Zhou, C.-S.; Wang, Y.-M.; Yan, N.; Wang, Y.-Y. Five solvent-induced cadmium coordination polymers (CPs) based on the same mixed ligands. *CrystEngComm* **2014**, *16*, 9560–9567.

Disclaimer/Publisher's Note: The statements, opinions and data contained in all publications are solely those of the individual author(s) and contributor(s) and not of MDPI and/or the editor(s). MDPI and/or the editor(s) disclaim responsibility for any injury to people or property resulting from any ideas, methods, instructions or products referred to in the content.